

Optimal Interval Observer for Discrete-Time Switched Systems

Haoran Zhang, Jun Huang^{ID}, *Member, IEEE*, Haochi Che^{ID}, and Zhengzhi Han

Abstract—The note is devoted to the interval observer design problem for discrete-time switched systems. By designing a suitable interval observer, it is convenient to achieve the interval estimation bounds of system states and reduce the effect of the unknown external disturbance. The interval observer design method has two main steps. They are H_∞ observer design and interval hull design respectively. Besides, the superiority of the proposed method is proved in the aspect of theory. One comparative example is carried out to verify the conclusion above.

Index Terms—Switched systems, H_∞ observer, interval hull.

I. INTRODUCTION

METHODS for interval estimation have been studied by researchers in the control theory field since the last century. With the development of control theory, many important observer design methods were proposed and the most famous of them were Luenberger observer [1] and Kalman filter [2]. It could be applied in various actual problems such as optimal control [3], fault diagnosis [4], stabilization problem [5], etc. The observers in the above works are actually a kind of asymptotic observers, that is, the recovered state can converge to the original state asymptotically. Based on this kind of observers, researchers studied the observer-based controller design problems [6]–[8]. A class of adaptive fuzzy observers were designed to deal with the inverse optimal output feedback control problem [6]. In [7], the adaptive neural network output feedback optimized control problem was considered. Neural networks were used to approximate the unknown internal dynamics and an adaptive state observer was employed to recover the original states. Besides, an asymptotic observer was employed in the finite-time containment control problem for nonlinear multiagent systems [8]. However, these observers can not satisfy the requirement for estimating uncertain systems. To solve the problem, Gouzé *et al.* firstly introduced the concept of interval observer (IO) and applied it in a population model with uncertainty [9]. Generally, the bounds of the population number could be effectively recovered with the application of IO. After that, the study on IO grew into a hot topic. In the previous work, the investigation mainly focused on finding observer gains to ensure the error dynamics nonnegative and ultimately uniformly bounded [10]. To expand the range of the application of IO,

some researchers applied it in nonlinear systems [11], [12]. Then, to relax the requirement of observer gains, the coordinate transformation method was employed in [13].

Switched systems (SSs) have a broad engineering background, such as reconfigurable optical add-drop multiplexer systems [14], flight control systems [15], power conversion systems [16] and so on. Although the stability problem for SSs has been widely discussed [17], [18], it is still difficult to estimate the state for systems with external disturbance. In this case, IO was introduced in SSs [19]–[21]. In [19], the authors applied the coordinate transformation method to IO for SSs. Different from the previous work, the authors in [20] designed an optimal IO based on the coordinate transformation method and improved the estimation accuracy effectively. However, as pointed out in [21], IO designed by coordinate transformation method may cause additional conservatism. On the other hand, set-membership method is also an effective method for interval estimation [22]–[24]. The states and disturbances are enclosed by the reachable set in this method. The reachable set usually can be described by ellipsoid, common polyhedron, zonotope and so on. Very recently, the zonotope-based method was applied to design an IO for SSs in [25]. It is worth noting that the order reduction calculation in [25] may increase the burden of the computation although the estimation accuracy was improved.

On the basis of the discussion above, the brief revisits the method of IO design problem for SSs. And an improved interval estimation method for SSs is proposed. The external disturbance is unknown but bounded. The method could be divided into two steps. The first step is to design an optimal H_∞ observer and the second one is to construct the interval hull for the system error estimation. The main contributions are as follows. (1) Compared with the existing works [20] and [25], the bounds obtained in this brief are tighter, and the sufficient conditions are also relaxed. (2) Different from [25], it is proved that the error bounds obtained are more accurate.

According to the descriptions above, the rest is organized as follows. Section II presents the necessary preliminaries. Section III explains the method of designing an optimal IO. In Section IV, a theoretical proof is made to illustrate the relationships among the proposed method, coordinate transformation method [20] and the zonotope-based method [25]. In Section V, to display the validity as well as superiority of the proposed method, an example is given.

Notations: \oplus represents the Minkowski sum. Given matrix $B \in R^{l_1 \times l_2}$, $B^+ = \max\{0, B\}$, $B^- = B^+ - B$ and $|B| = B^- + B^+$. Given a real symmetric matrix $B \in R^{n \times n}$, $B \succ 0$ ($B \prec 0$) represents that B is positive (negative) definite. The symbol \emptyset represents a set with no element.

II. SYSTEM DESCRIPTION AND PRELIMINARIES

Consider the following SS:

Manuscript received July 4, 2021; accepted July 27, 2021. Date of publication August 2, 2021; date of current version March 15, 2022. This work was supported by the National Natural Science Foundation of China under Grant 61403267. This brief was recommended by Associate Editor Z. Galias. (Corresponding author: Jun Huang.)

Haoran Zhang, Jun Huang, and Haochi Che are with the School of Mechanical and Electrical Engineering, Soochow University, Suzhou 215131, China (e-mail: cauchyhot@163.com).

Zhengzhi Han is with the School of Electronic, Information and Electrical Engineering, Shanghai Jiaotong University, Shanghai 200240, China.

Color versions of one or more figures in this article are available at <https://doi.org/10.1109/TCSII.2021.3101585>.

Digital Object Identifier 10.1109/TCSII.2021.3101585

1549-7747 © 2021 IEEE. Personal use is permitted, but republication/redistribution requires IEEE permission.

See <https://www.ieee.org/publications/rights/index.html> for more information.

$$\begin{cases} x(k+1) = A_{p(k)}x(k) + B_{p(k)}u(k) + E_{p(k)}v(k), \\ y(k) = C_{p(k)}x(k), \end{cases} \quad (1)$$

where $x(k) \in R^n$ is the state, $u(k) \in R^m$ is the input, $y(k) \in R^q$ is the output, and $v(k) \in R^s$ is the disturbance with known bounds \bar{v} and \underline{v} , which satisfies $v \in [\underline{v}, \bar{v}]$. $p(k)$ is the switching signal of the system, and $p(k) = \sigma \in S$, $S = \{1, \dots, N\}$, where N is the number of subsystems. The matrices A_σ , B_σ , C_σ and E_σ are all known. For the sake of simplicity, the step k is omitted when it is not necessary.

Remark 1: For discrete-time SSs and general continuous-time systems, there are two main differences between them. Firstly, SSs are different from general systems. SSs are a class of hybrid systems with some subsystems, which can be activated by a switching law. Whereas, general systems are always in single mode. Secondly, discrete-time systems are different from continuous-time systems. Discrete-time systems use discrete step-size signals while continuous-time systems use the continuous analog signals.

Remark 2: System (1) can be used to describe a flight control system and a switched-capacitor converter system, such as [15] and [26]. The flight control system can be viewed as a switched system since the separated dynamical system is determined by a specific separation law [15]. In [26], a DC-DC converter can be transformed into a switched system because its circuit model behaves the switching phenomenon.

The observer of system (1) is given as

$$\hat{x}(k+1) = (A_\sigma - L_\sigma C_\sigma)\hat{x}(k) + B_\sigma u(k) + L_\sigma y(k), \quad (2)$$

where $\hat{x}(k) \in R^n$ is the state estimation for system (1) and $L_{p(k)} \in R^{n \times q}$ is the observer gain. The error dynamics is

$$e(k+1) = (A_\sigma - L_\sigma C_\sigma)e(k) + E_\sigma v(k), \quad (3)$$

where $e = x - \hat{x}$.

Proposition 1 [25]: Given constants $\alpha > 1$ and $0 < \beta < 1$. If there exist $\gamma > 0$ and matrices $P_i = P_i^T \in R^{n \times n} > 0$, $P_j = P_j^T \in R^{n \times n} > 0$, $\forall i, j \in S$, $i \neq j$ such that

$$\begin{cases} \text{minimize } \gamma \\ \text{subject to:} \\ \begin{bmatrix} -\beta P_i + I_n & * & * \\ E_i^T P_i A_i - E_i^T U_i C_i & E_i^T P_i E_i - \gamma I & * \\ P_i A_i - U_i C_i & 0 & -P_i \end{bmatrix} < 0, \\ P_i < \alpha P_j, \\ \frac{1}{\tau_a} + \frac{\ln \beta}{\ln \alpha} < 0, \end{cases} \quad (4)$$

where $L_i = P_i^{-1} U_i$ and τ_a is the average dwell time (ADT) (See [27, Definition 1]), then (2) is an optimal H_∞ observer (See the H_∞ performance in [27]).

III. INTERVAL HULL DESIGN METHOD

In this part, a novel method is presented to realize the interval estimation of system (1). Some definitions for interval hull technique are given firstly.

Property 1: For a zonotope defined in [22], it has the following properties:

$$\begin{aligned} \langle c_1, H_1 \rangle \oplus \langle c_2, H_2 \rangle &= \langle c_1 + c_2, [H_1 \ H_2] \rangle, \\ L \langle c_1, H_1 \rangle &= \langle Lc_1, LH_1 \rangle, \end{aligned}$$

where c_1 and c_2 are the centers of the two zonotopes, H_1 and H_2 are the shape matrices of them.

Lemma 1: For zonotope $\langle c, H \rangle$ with $c \in R^p$, $H \in R^{p \times q}$, it has corresponding matrix $\bar{H} \in R^{p \times p}$, satisfying $\langle c, H \rangle \subseteq \langle c, \bar{H} \rangle$, where \bar{H} is a diagonal matrix with

$$\bar{H}_{m,m} = \sum_{i=1}^q |H_{m,i}|, \quad i = 1, 2, \dots, p,$$

i.e.,

$$\bar{H} = \begin{bmatrix} \sum_{i=1}^q |H_{1,i}| & \dots & 0 \\ \vdots & \ddots & \vdots \\ 0 & \dots & \sum_{i=1}^q |H_{p,i}| \end{bmatrix}.$$

Assumption 1: The initial state x_0 and the disturbance $v(k)$ are bounded, i.e.,

$$\begin{aligned} x_0 &\in \langle c(0), H(0) \rangle = X_0, \\ v(k) &\in \langle 0, H_v \rangle = W, \\ e(k) &\in \langle 0, H(k) \rangle = \Lambda(k), \end{aligned} \quad (5)$$

where $H(0)$ is known and $H_v = \text{diag}(\bar{v})$.

Definition 1: The interval vector $A \in R^m$ is considered as the interval hull of zonotope Z

$$A = [d, e] = \text{Box}(Z), \quad (6)$$

where $d = [d_1, d_2, \dots, d_m]^T$ and $e = [e_1, e_2, \dots, e_m]^T$.

Definition 2: Given a zonotope $A \subset R^m$, the box of it is considered as the smallest interval vector containing A . The relationship between them is as follows:

$$A \subset \text{Box}(A) = [d, e], \quad (7)$$

with $d = [d_1, d_2, \dots, d_m]^T$ and $e = [e_1, e_2, \dots, e_m]^T$.

Lemma 2: For an i -dimensional column vector χ and a matrix $H \in R^{i \times i}$, if there exists $\underline{\chi}$ and $\bar{\chi}$ such that $\underline{\chi} \leq \chi \leq \bar{\chi}$, then

$$H^+ \underline{\chi} - H^- \bar{\chi} \leq H \chi \leq H^+ \bar{\chi} - H^- \underline{\chi}. \quad (8)$$

Lemma 3: Given $G = [d, e] \subset R^n$ and $A \in R^{m \times n} \geq 0$, we have

$$\text{Box}(AG) = AG = [Ad, Ae].$$

Theorem 1: For the error dynamics (3), the error $e(k)$ has the upper bound \bar{e} and the lower bound \underline{e} , which make up the following interval vector $[\underline{e}(k), \bar{e}(k)]$

$$\begin{aligned} [\underline{e}(k), \bar{e}(k)] &= \text{Box}((\prod_{i=0}^{k-1} B_{p(i)}) \Lambda(0)) \\ &\oplus \bigoplus_{i=0}^{k-1} \text{Box}((\prod_{j=i}^{k-1} B_{p(j)}) B_{p(i)}^{-1} E_{p(i)} W), \end{aligned} \quad (9)$$

where

$$\begin{aligned} B_{p(i)} &= A_{p(i)} - L_{p(i)} C_{p(i)}, \\ \prod_{j=i}^{k-1} B_{p(j)} &= B_{p(k-1)} B_{p(k-2)} \dots B_{p(i)}. \end{aligned} \quad (10)$$

Proof: According to Assumption 1 and Definition 1, the initial error is $[\underline{e}(0), \bar{e}(0)] = \text{Box}(\Lambda(0))$.

Considering (3) and (5), when $k = 0$, we have

$$\Lambda(1) = B_{p(0)} \Lambda(0) \oplus E_{p(0)} W.$$

When $k = 1$, one can obtain

$$\Lambda(2) = B_{p(1)} \Lambda(1) \oplus E_{p(1)} W$$

Algorithm 1 Interval Estimation by Interval Hull-Based Method**In:** $\hat{x}(0)$, W , X_0 , y , u ;**Out:** \underline{x} , \bar{x} ;1: **Given initial values:**2: $\hat{x}(0) = x(0) = c(0)$, $e(0) \in \Lambda_0$, $v \in W$, $D_{v(0)} = E_{p(0)}W$;3: $M_{x(0)} = \langle 0, H(0) \rangle$, $M_{v(0)} = \emptyset$;4: **for** $i \geq 0$ **do**5: $[\underline{e}(i+1), \bar{e}(i+1)] = \text{Box}(M_{x(i)} \oplus M_{v(i)})$ 6: $\bar{x}(i) = \hat{x}(i) + \bar{e}(i)$, $\underline{x}(i) = \hat{x}(i) + \underline{e}(i)$ 7: $\hat{x}(i+1) = (A_\sigma - L_\sigma C_\sigma)\hat{x}(i) + B_\sigma u(i) + L_\sigma y(i)$ 8: $M_{x(i+1)} = (A_{p(i)} - L_{p(i)}C_{p(i)})M_{x(i)}$ 9: $M_{v(i+1)} = M_{v(i)} \oplus \text{Box}(D_{v(i)})$ 10: $D_{v(i+1)} = (A_{p(i)} - L_{p(i)}C_{p(i)})D_{v(i)}$ 11: **end for**

$$= B_{p(1)}B_{p(0)}\Lambda(0) \oplus B_{p(1)}E_{p(0)}W \oplus E_{p(1)}W. \quad (11)$$

Then, repeating the above steps, we have

$$\Lambda(k+1) = \left(\prod_{i=0}^k B_{p(i)}\right)\Lambda(0) \oplus \bigoplus_{i=0}^k \left(\prod_{j=i}^k B_{p(j)}\right)B_{p(i)}^{-1}E_{p(i)}W. \quad (12)$$

From Definition 1, the set $\Lambda(k)$ is described by the following interval hull

$$[\underline{e}(k), \bar{e}(k)] = \text{Box}(\Lambda(k)) = \text{Box}\left(\left(\prod_{i=0}^{k-1} B_{p(i)}\right)X_0\right) \oplus \bigoplus_{i=0}^{k-1} \text{Box}\left(\left(\prod_{j=i}^{k-1} B_{p(j)}\right)B_{p(i)}^{-1}E_{p(i)}W\right). \quad (13)$$

Consider the H_∞ observer (2), and the structure of the interval hull-based observer is

$$\begin{cases} \bar{x} = \bar{e} + \hat{x}, \\ \underline{x} = \underline{e} + \hat{x}, \end{cases} \quad (14)$$

where $[\underline{e}, \bar{e}]$ is given in Theorem 1. According to (9), Theorem 1 could be realized by the following iterative algorithm.

IV. RELATIONSHIPS AND COMPARISONS BETWEEN THE METHODS

In this part, the proposed method would make comparisons with the coordinate transformation and zonotope-based methods, respectively.

Proposition 2 [20]: Denote $z(k) = R_\sigma x(k)$, then system (1) can be converted as follows:

$$\begin{cases} z(k+1) = R_\sigma A_\sigma R_\sigma^{-1}z(k) + R_\sigma B_\sigma u(k) + R_\sigma v(k), \\ y(k) = C_\sigma R_\sigma^{-1}z(k). \end{cases} \quad (15)$$

For the system (15), the structure of the IO designed by the coordinate transformation method is given by

$$\begin{cases} \bar{z}(k+1) = P_\sigma \bar{z}(k) + R_\sigma B_\sigma u(k) + |R_\sigma| \bar{v}(k) + R_\sigma L_\sigma y(k), \\ \underline{z}(k+1) = P_\sigma \underline{z}(k) + R_\sigma B_\sigma u(k) + |R_\sigma| \underline{v}(k) + R_\sigma L_\sigma y(k), \\ \bar{x}^c(k) = (R_\sigma^{-1})^+ \bar{z}(k) - (R_\sigma^{-1})^- \underline{z}(k), \\ \underline{x}^c(k) = (R_\sigma^{-1})^+ \underline{z}(k) - (R_\sigma^{-1})^- \bar{z}(k), \end{cases} \quad (16)$$

where $P_\sigma = R_\sigma(A_\sigma - L_\sigma C_\sigma)R_\sigma^{-1}$, R_σ is the transformation matrix. \underline{x}^c and \bar{x}^c are the bounds of system (1). For convenience, the coordinate transformation method is called as method 1.

A. Theoretical Comparative Analysis Between the Method 1 and Algorithm 1

Theorem 2: For the observers (14) and (16), given the same conditions (including observer gains and initial states), the following inequations hold

$$\begin{cases} \bar{x}^c \geq \bar{x}, \\ \underline{x}^c \leq \underline{x}, \end{cases} \quad (17)$$

where $[\underline{x}^c, \bar{x}^c]$ is given by the observer (16), and $[\underline{x}, \bar{x}]$ is generated from the observer (14).**Proof:** For the system (15), the observer is designed as

$$\hat{z}(k+1) = P_\sigma \hat{z}(k) + R_\sigma B_\sigma u(k) + R_\sigma L_\sigma y(k). \quad (18)$$

Substituting $\hat{z}(0) = R_{\sigma(0)}\hat{x}(0)$ into (18) and using iterative algorithm, it could be obtained that

$$\hat{x} = R_\sigma^{-1}\hat{z}, \quad (19)$$

Define $e^z = z - \hat{z}$, according to $z = R_\sigma x$ and (19), one can get that

$$e^z = R_\sigma e. \quad (20)$$

If Λ^z represents the reachable set of e^z , then it follows from (20) that $\Lambda^z = R_\sigma \Lambda$. Denote $\text{Box}(\Lambda^z) = [\underline{\omega}^z, \bar{\omega}^z]$, then

$$\underline{\omega}^z \leq e^z \leq \bar{\omega}^z. \quad (21)$$

Define that

$$\begin{cases} \bar{e}^z = \bar{z} - \hat{z}, \\ \underline{e}^z = \underline{z} - \hat{z}. \end{cases} \quad (22)$$

Substituting (16) and (18) into (22) gives that

$$\begin{cases} \bar{e}^z(k+1) = P_\sigma \bar{e}^z(k) + |R_\sigma| \bar{v}(k) \\ \quad = (\prod_{i=0}^k P_{p(i)})\bar{e}^z(0) + \sum_{i=0}^k (K_{p(i)}|R_{p(i)}|\bar{v}(i)), \\ \underline{e}^z(k+1) = P_\sigma \underline{e}^z(k) + |R_\sigma| \underline{v}(k) \\ \quad = (\prod_{i=0}^k P_{p(i)})\underline{e}^z(0) + \sum_{i=0}^k (K_{p(i)}|R_{p(i)}|\underline{v}(i)), \end{cases} \quad (23)$$

where

$$K_{p(i)} = \left(\prod_{j=i}^{k-1} P_{p(j)}\right)P_{p(i)}^{-1}.$$

Considering Lemma 3, define $\text{Box}(\tilde{\Lambda}^z) = [\underline{e}^z, \bar{e}^z]$, then

$$\begin{aligned} \text{Box}(\tilde{\Lambda}^z(k+1)) &= \text{Box}\left(\left(\prod_{i=0}^k P_{p(i)}\right)\text{Box}(\Lambda^z(0))\right) \\ &\quad \oplus \bigoplus_{i=0}^k \text{Box}(K_{p(i)}|R_{p(i)}|\text{Box}(W)). \end{aligned} \quad (24)$$

In view of $\Lambda^z(k) = R_\sigma \Lambda(k)$, (13) is equivalent to

$$\begin{aligned} \text{Box}(\Lambda^z(k+1)) &= \text{Box}\left(\left(\prod_{i=0}^k P_{p(i)}\right)\Lambda^z(0)\right) \\ &\quad \oplus \bigoplus_{j=0}^k \text{Box}(K_{p(i)}R_{p(j)}W). \end{aligned} \quad (25)$$

Since

$$\begin{cases} \Lambda^z(0) \subseteq \text{Box}(\Lambda^z(0)), \\ W \subseteq \text{Box}(W), \\ |R_\sigma| \geq R_\sigma, \end{cases}$$

comparing (24) with (25) deduces that $\text{Box}(\Lambda^z) \subseteq \text{Box}(\tilde{\Lambda}^z)$.

Then, the following inequalities hold

$$\begin{cases} \bar{e}^z \geq \bar{\omega}^z, \\ \underline{e}^z \leq \underline{\omega}^z, \end{cases} \quad (26)$$

and from (20) and (21), we have

$$\underline{e}^z \leq R_\sigma e \leq \bar{e}^z. \quad (27)$$

Define the parallelotope \tilde{Q} as the set of $e(k)$ with the constraint of (27). From (21), it follows that $\underline{\omega}^z \leq R_\sigma e \leq \bar{\omega}^z$, then define a new parallelotope Q as the set of $e(k)$ described by it. According to (26), we have $Q \subseteq \tilde{Q}$. Since $\Lambda(k)$ is the reachable set, one can get that

$$\Lambda(k) \subseteq Q \subseteq \tilde{Q}. \quad (28)$$

For $i \geq 1$, the following equalities hold

$$\begin{cases} \bar{x}^c(i) = (R_\sigma^{-1})^+ \bar{z}(i) - (R_\sigma^{-1})^- \underline{z}(i), \\ \underline{x}^c(i) = (R_\sigma^{-1})^+ \underline{z}(i) - (R_\sigma^{-1})^- \bar{z}(i). \end{cases} \quad (29)$$

Denote $\bar{e}^c = \bar{x}^c - \hat{x}$ and $\underline{e}^c = \underline{x}^c - \hat{x}$, then

$$\begin{cases} \bar{x}^c = \bar{e}^c + \hat{x}, \\ \underline{x}^c = \underline{e}^c + \hat{x}. \end{cases} \quad (30)$$

From (19), \hat{x} could be transformed into

$$\hat{x} = R_\sigma^{-1} \hat{z} = (R_\sigma^{-1})^+ \hat{z} - (R_\sigma^{-1})^- \hat{z}. \quad (31)$$

From (30), we have $\bar{e}^c = \bar{x}^c - \hat{x}$ and $\underline{e}^c = \underline{x}^c - \hat{x}$. Substituting (29) and (31) into them yields

$$\begin{cases} \bar{e}^c = (R_\sigma^{-1})^+ (\bar{z}^c - \hat{z}) - (R_\sigma^{-1})^- (\underline{z}^c - \hat{z}), \\ \underline{e}^c = (R_\sigma^{-1})^+ (\underline{z}^c - \hat{z}) - (R_\sigma^{-1})^- (\bar{z}^c - \hat{z}). \end{cases}$$

Considering (22), it could be converted into

$$\begin{cases} \bar{e}^c = (R_\sigma^{-1})^+ \bar{e}^z - (R_\sigma^{-1})^- \underline{e}^z, \\ \underline{e}^c = (R_\sigma^{-1})^+ \underline{e}^z - (R_\sigma^{-1})^- \bar{e}^z. \end{cases} \quad (32)$$

In view of Lemma 2, one can get

$$(R_\sigma^{-1})^+ \underline{e}^z - (R_\sigma^{-1})^- \bar{e}^z \leq R_\sigma^{-1} e^z \leq (R_\sigma^{-1})^+ \bar{e}^z - (R_\sigma^{-1})^- \underline{e}^z.$$

It follows from (20) and (32) that

$$\underline{e}^c \leq e \leq \bar{e}^c. \quad (33)$$

Due to $e(k) \in \tilde{Q}$, we have

$$[\underline{e}^c, \bar{e}^c] = \text{Box}(\tilde{Q}). \quad (34)$$

In addition, it follows from (28) that

$$\text{Box}(\Lambda(k)) \subseteq \text{Box}(\tilde{Q}). \quad (35)$$

Because of $\text{Box}(\Lambda) = [\underline{e}, \bar{e}]$, we have

$$[\underline{e}, \bar{e}] \subseteq [\underline{e}^c, \bar{e}^c], \quad (36)$$

i.e.,

$$\begin{cases} \bar{e}^c \geq \bar{e}, \\ \underline{e}^c \leq \underline{e}. \end{cases} \quad (37)$$

Finally, from (14), (30) and (37), it is concluded that

$$\begin{cases} \bar{x}^c = \hat{x} + \bar{e}^c \geq \hat{x} + \bar{e} = \bar{x}, \\ \underline{x}^c = \hat{x} + \underline{e}^c \leq \hat{x} + \underline{e} = \underline{x}. \end{cases} \quad (38)$$

Proposition 3 [25]: For the system (1), zonotope $\langle \hat{x}(k), H(k) \rangle$ can include the state $x(k)$ totally, where $H(k)$ satisfies:

$$H(k+1) = [(A_\sigma - L_\sigma C_\sigma) \bar{H}(k), E_\sigma H_v], \quad (39)$$

and $\bar{H}(k)$ is introduced in Lemma 1.

Define $\text{Box}(\langle \hat{x}, H \rangle) = [\underline{x}^{zo}, \bar{x}^{zo}]$. From [24, Property 4], the bounds of state is as follows

$$\begin{cases} \bar{x}_i^{zo}(k) = \hat{x}_i(k) + \sum_{j=1}^q |H_{i,j}(k)|, \\ \underline{x}_i^{zo}(k) = \hat{x}_i(k) - \sum_{j=1}^q |H_{i,j}(k)|, \end{cases} \quad (40)$$

where $i = 1, \dots, n$. For convenience, the zonotope-based method is called as method 2.

B. Theoretical Comparative Analysis Between the Method 2 and Algorithm 1

Theorem 3: For the observers (14) and (40), given the same observer gains and the same initial states as in Theorem 2, the following equations hold

$$\begin{cases} \bar{x}^{zo} \geq \bar{x}, \\ \underline{x}^{zo} \leq \underline{x}, \end{cases} \quad (41)$$

where $[\underline{x}^{zo}, \bar{x}^{zo}]$ is given by the observer (40), and $[\underline{x}, \bar{x}]$ is given by the observer (14).

Proof: Define $\Lambda^{zo}(k) = \langle 0, H(k) \rangle$ and $\bar{\Lambda}^{zo}(k) = \langle 0, \bar{H}(k) \rangle$. According to (39) and Property 1, it follows that

$$\begin{aligned} \Lambda^{zo}(k+1) &= \langle 0, H(k+1) \rangle \\ &= \langle 0, (A_\sigma - L_\sigma C_\sigma) \bar{H}(k) \rangle \oplus \langle 0, E_\sigma H_v \rangle \\ &= (A_\sigma - L_\sigma C_\sigma) \langle 0, \bar{H}(k) \rangle \oplus E_\sigma \langle 0, H_v \rangle \\ &= (A_\sigma - L_\sigma C_\sigma) \bar{\Lambda}^{zo}(k) \oplus E_\sigma W. \end{aligned} \quad (42)$$

Since $\bar{\Lambda}^{zo}(k) \supseteq \Lambda^{zo}(k)$ and $\Lambda^{zo}(0) = \Lambda(0)$, from (42), one has

$$\begin{aligned} \Lambda^{zo}(k+1) &\supseteq (A_\sigma - L_\sigma C_\sigma) \Lambda^{zo}(k) \oplus E_\sigma W \\ &= \left(\prod_{i=0}^k B_{p(i)} \right) \Lambda(0) \oplus \bigoplus_{i=0}^k \left(\left(\prod_{j=i}^k B_{p(j)} \right) B_{p(i)}^{-1} E_{p(i)} W \right) \\ &= \Lambda(k+1). \end{aligned} \quad (43)$$

It follows from (43) that $\text{Box}(\Lambda^{zo}(k)) \supseteq \text{Box}(\Lambda(k))$. Since $\text{Box}(\Lambda^{zo}) = [\underline{v}^{zo}, \bar{v}^{zo}]$ and $\text{Box}(\Lambda) = [\underline{e}, \bar{e}]$, it can be deduced that

$$\begin{cases} \bar{v}^{zo} \geq \bar{e}, \\ \underline{v}^{zo} \leq \underline{e}. \end{cases} \quad (44)$$

Thus, the following inequalities hold

$$\begin{cases} \bar{x}^z = \hat{x} + \bar{v}^{zo} \geq \hat{x} + \bar{e} = \bar{x}, \\ \underline{x}^z = \hat{x} + \underline{v}^{zo} \leq \hat{x} + \underline{e} = \underline{x}. \end{cases} \quad (45)$$

V. SIMULATION

Consider a circuit system borrowed from [28], and the “on” and “off” of switch S determine the switched signal. According to the parameters in [28], the system matrices of (1) are as follows

$$\begin{aligned} A_1 &= \begin{bmatrix} -33.3 & 0 \\ 0 & -412.5 \end{bmatrix}, A_2 = \begin{bmatrix} -40.7 & -36.7 \\ 82.5 & -412.5 \end{bmatrix}, \\ B_1 &= B_2 = \begin{bmatrix} 37.0 \\ 0.0 \end{bmatrix}, E_1 = \begin{bmatrix} -0.12 \\ 0.21 \end{bmatrix}, \\ C_1 &= C_2 = [0 \quad 1], E_2 = \begin{bmatrix} -0.14 \\ 0.23 \end{bmatrix}. \end{aligned}$$

TABLE I
RESULT OF THE SIMULATION

	method 1	method 2	method 3
interval width of x_1	0.76	0.32	0.20
interval width of x_2	1.16	0.65	0.11

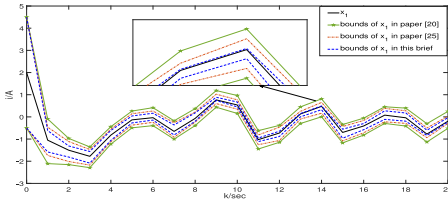


Fig. 1. The state x_1 and its bounds by three methods.

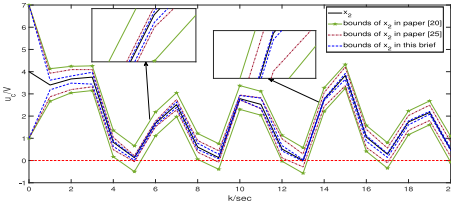


Fig. 2. The state x_2 and its bounds by three methods.

Given constants $\beta = 0.33$ and $\alpha = 2.28$, solving the LMIs in (4), we obtain

$$\gamma = 0.2221, \quad L_1 = \begin{bmatrix} 0.0017 \\ -4.1251 \end{bmatrix}, \quad L_2 = \begin{bmatrix} -0.3650 \\ -4.5376 \end{bmatrix}.$$

The simulation results are shown in Fig. 1 and Fig. 2. x_1 represents the current i flowing out of the power supply V_{in} , while x_2 represents the voltage u_C of the capacitor C .

In the simulation, three methods are compared with each other. Algorithm 1 is considered as method 3 here. With the same conditions, more accurate interval estimations are obtained by the interval hull-based method, compared with the other two methods. Table I shows the result in the form of data. From Table I, it can be seen that the width of method 3 is tighter than that of method 1 and 2 clearly.

Remark 3: In [28], the circuit system is a continuous-time system. The difference between a discrete-time system and a continuous-time system is that one uses the continuous analog signal while the other one uses the discrete step-size signal. In the simulation, the discretization algorithm is used to transform the continuous-time system into a discrete-time system.

VI. CONCLUSION

This brief presents an improved interval estimation method for discrete-time SSs. This method combines the H_∞ observer with the interval hull. The H_∞ technique makes the observer against interference and the interval hull depends on reachability analysis technique. Compared with the coordinate transformation method, the proposed method reduces the additional conservatism. Different from the zonotope-based method, the interval hull-based method has higher computational efficiency and achieves more accurate estimation. In simulation, a circuit model is used to illustrate the previous conclusion and the simulation result verifies the relationship among the three methods. In the nearly future, the interval observer-based controller design problem for SSs will be investigated.

REFERENCES

- [1] D. Luenberger, "Observers for multivariable systems," *IEEE Trans. Autom. Control*, vol. 11, no. 2, pp. 190–197, Apr. 1966.
- [2] R. E. Kalman, "A new approach to linear filtering and prediction problems," *J. Basic Eng.*, vol. 82, no. 1, pp. 35–45, 1960.
- [3] Y. Li, K. Sun, and S. Tong, "Observer-based adaptive fuzzy fault-tolerant optimal control for SISO nonlinear systems," *IEEE Trans. Cybern.*, vol. 49, no. 2, pp. 649–661, Feb. 2019.
- [4] X. Liu, X. Gao, and J. Han, "Observer-based fault detection for high-order nonlinear multi-agent systems," *J. Franklin Inst.*, vol. 353, no. 1, pp. 72–94, 2016.
- [5] J. Alipoor, Y. Miura, and T. Ise, "Power system stabilization using virtual synchronous generator with alternating moment of inertia," *IEEE J. Emerg. Sel. Topics Power Electron.*, vol. 3, no. 2, pp. 451–458, Jun. 2015.
- [6] Y. Li, X. Min, and S. Tong, "Observer-based fuzzy adaptive inverse optimal output feedback control for uncertain nonlinear systems," *IEEE Trans. Fuzzy Syst.*, vol. 29, no. 6, pp. 1484–1495, Jun. 2021.
- [7] Y. Li, Y. Liu, and S. Tong, "Observer-based neuro-adaptive optimized control of strict-feedback nonlinear systems with state constraints," *IEEE Trans. Neural Netw. Learn. Syst.*, early access, Jan. 26, 2021, doi: [10.1109/TNNLS.2021.3051030](https://doi.org/10.1109/TNNLS.2021.3051030).
- [8] Y. Li, F. Qu, and S. Tong, "Observer-based fuzzy adaptive finite-time containment control of nonlinear multiagent systems with input delay," *IEEE Trans. Cybern.*, vol. 51, no. 1, pp. 126–137, Jan. 2021.
- [9] J. L. Gouzé, A. Rapaport, and M. Z. Hadj-Sadok, "Interval observers for uncertain biological systems," *Ecol. Model.*, vol. 133, nos. 1–2, pp. 45–56, 2000.
- [10] L. Farina and S. Rinaldi, *Positive Linear Systems: Theory and Applications*. New York, NY, USA: Wiley, 2000.
- [11] D. Efimov, T. Raïssi, and A. Zolghadri, "Control of nonlinear and LPV systems: Interval observer-based framework," *IEEE Trans. Autom. Control*, vol. 58, no. 3, pp. 773–778, Mar. 2013.
- [12] T. Raïssi, G. Videau, and A. Zolghadri, "Interval observer design for consistency checks of nonlinear continuous-time systems," *Automatica*, vol. 46, no. 3, pp. 518–527, 2010.
- [13] F. Mazenc and O. Bernard, "Interval observers for linear time-invariant systems with disturbances," *Automatica*, vol. 47, no. 1, pp. 140–147, 2011.
- [14] W. Mo, C. Gutterman, Y. Li, S. Zhu, Z. Gil, and D. Kilper, "Deep-neural-network-based wavelength selection and switching in ROADMs systems," *J. Opt. Commun. Netw.*, vol. 10, no. 10, pp. D1–D11, 2018.
- [15] L. Xu, Q. Wang, W. Li, and Y. Hou, "Stability analysis and stabilisation of full-envelope networked flight control systems: Switched system approach," *IET Control Theory Appl.*, vol. 6, no. 2, pp. 286–296, 2012.
- [16] D. Y. Jung *et al.*, "Design and evaluation of cascode GaN FET for switching power conversion systems," *ETRI J.*, vol. 39, no. 1, pp. 62–68, 2017.
- [17] Y.-E. Wang, H. R. Karimi, and D. Wu, "Conditions for the stability of switched systems containing unstable subsystems," *IEEE Trans. Circuits Syst. II, Exp. Briefs*, vol. 66, no. 4, pp. 617–621, Apr. 2019.
- [18] S. Du, H. R. Karimi, J. Qiao, D. Wu, and C. Feng, "Stability analysis for a class of discrete-time switched systems with partial unstable subsystems," *IEEE Trans. Circuits Syst. II, Exp. Briefs*, vol. 66, no. 12, pp. 2017–2021, Dec. 2019.
- [19] S. Guo and F. Zhu, "Interval observer design for discrete-time switched system," *IFAC-PapersOnLine*, vol. 50, no. 1, pp. 5073–5078, 2017.
- [20] T. Dinh, G. Marouani, T. Raïssi, Z. Wang, and H. Messaoud, "Optimal interval observers for discrete-time linear switched systems," *Int. J. Control*, vol. 93, pp. 2613–2621, Feb. 2019.
- [21] E. Chambon, L. Burlion, and P. Apkarian, "Overview of linear time-invariant interval observer design: Towards a non-smooth optimisation-based approach," *IET Control Theory Appl.*, vol. 10, no. 11, pp. 1258–1268, 2016.
- [22] T. Alamo, J. M. Bravo, and E. F. Camacho, "Guaranteed state estimation by zonotopes," *Automatica*, vol. 41, no. 6, pp. 1035–1043, 2005.
- [23] C. Combastel, "Zonotopes and Kalman observers: Gain optimality under distinct uncertainty paradigms and robust convergence," *Automatica*, vol. 55, pp. 265–273, May 2015.
- [24] W. Tang, Z. Wang, Y. Wang, T. Raïssi, and Y. Shen, "Interval estimation methods for discrete-time linear time-invariant systems," *IEEE Trans. Autom. Control*, vol. 64, no. 11, pp. 4717–4724, Nov. 2019.
- [25] J. Huang, X. Ma, H. Che, and Z. Han, "Further result on interval observer design for discrete-time switched systems and application to circuit systems," *IEEE Trans. Circuits Syst. II, Exp. Briefs*, vol. 67, no. 11, pp. 2542–2546, Nov. 2020.
- [26] M. D. Seeman and S. R. Sanders, "Analysis and optimization of switched-capacitor DC–DC converters," *IEEE Trans. Power Electron.*, vol. 23, no. 2, pp. 841–851, Mar. 2008.
- [27] W. Xiang, J. Xiao, and M. N. Iqbal, "Robust observer design for nonlinear uncertain switched systems under asynchronous switching," *Nonlinear Anal. Hybrid Syst.*, vol. 6, no. 1, pp. 754–773, 2012.
- [28] S. Banerjee and K. Chakrabarty, "Nonlinear modeling and bifurcations in the boost converter," *IEEE Trans. Power Electron.*, vol. 13, no. 2, pp. 252–260, Mar. 1998.